Semantic Annotation of Soccer Videos: Automatic Highlights Identification

5 authors, including:

Jurgen Assfalg
Città Metropolitana di Firenze
53 PUBLICATIONS   **968** CITATIONS

SEE PROFILE

Marco Bertini
University of Florence
223 PUBLICATIONS   **3,544** CITATIONS

SEE PROFILE

Carlo Colombo
University of Florence
133 PUBLICATIONS   **2,029** CITATIONS

SEE PROFILE

Alberto Del Bimbo
University of Florence
670 PUBLICATIONS   **13,416** CITATIONS

SEE PROFILE

Some of the authors of this publication are also working on these related projects:

Project   Thermal object detector on high-speed railway View project

Project   3D Shape Analysis and recognition on the mesh manifold View project

Semantic annotation of soccer videos: automatic highlights identification

Jürgen Assfalg,[*] Marco Bertini, Carlo Colombo, Alberto Del Bimbo, and Walter Nunziati

Dipartimento di Sistemi e Informatica, Via S. Marta 3, Firenze 50139, Italy

Abstract

Automatic semantic annotation of video streams allows both to extract significant clips for production logging and to index video streams for posterity logging. Automatic annotation for production logging is particularly demanding, as it is applied to non-edited video streams and must rely only on visual information. Moreover, annotation must be computed in quasi real-time. In this paper, we present a system that performs automatic annotation of the principal highlights in soccer video, suited for both production and posterity logging. The knowledge of the soccer domain is encoded into a set of finite state machines, each of which models a specific highlight. Highlight detection exploits visual cues that are estimated from the video stream, and particularly, ball motion, the currently framed playfield zone, players' positions and colors of players' uniforms. The highlight models are checked against the current observations, using a model checking algorithm. The system has been developed within the EU ASSAVID project.
© 2003 Elsevier Inc. All rights reserved.

Keywords: Semantic annotation; Sports videos; Highlights detection

1. Introduction

Video annotation and retrieval by content are motivated by the huge amount of video daily produced both by broadcasters and individual film shooters. In particu-

---

[*] Corresponding author.
E-mail addresses: assfalg@dsi.unifi.it (J. Assfalg), bertini@dsi.unifi.it (M. Bertini), colombo@dsi.unifi.it (C. Colombo), delbimbo@dsi.unifi.it (A. Del Bimbo), nunziati@dsi.unifi.it (W. Nunziati).

lar, broadcasters are strongly interested in tools that enable to log the most relevant shots of a video stream with annotations that may support effectively the task of editing TV programmes. Annotations should include the description of the most relevant highlights and other in-depth information. Making the annotation as much as possible automatic is one of the best ways to improve the production quality and to face a competitive market. To this end, broadcasters employ two distinct logging approaches. In *production logging*, which is carried out live or shortly after the event, the assistant producer selects manually the relevant shots to be included into the programme of the day. In *posterity logging*, the video material is catalogued for later reuse. In this case, librarians typically prepare a detailed textual annotation of each video tape after a careful inspection of its content. As a result of that, annotations strongly depend on which of the two logging approaches is followed. In particular, production logging typically deals with raw video—captions and effects like replays that are useful for automatic annotation are added later during the editing phase, and speech and audio are available only occasionally. On the other hand, in posterity logging, automatic annotation can use speech and audio as well as captions and editing effects to extract semantic information from the video stream. Besides, while in production logging the annotation must be performed on-line to meet the nearly real-time requirements of *as live* [1] programme production, in posterity logging the annotation can be performed off-line.

Although there is an extensive literature on the subject of automatic video annotation for video archiving, this distinction and its implications have never been considered. Proposals have been concerned with solutions of general applicability, addressing detection of syntactic features like editing effects and keyframes [1,10,12,16,28] as well as with solutions for the extraction of video semantics, specifically tailored to particular application domains [5,6,9,17,19,25].

In the specific case of sports videos, automatic semantic annotation requires that the most relevant highlights are identified. Sports highlights represent atomic entities at the semantic level. They have a limited temporal extension and a relatively simple structure, that can be modelled as the spatio-temporal concatenation of specific events. The challenge in sports highlight detection is therefore tied with the choice of appropriate representation models and the selection of meaningful cues that can be extracted from the video stream. Typical facts of tennis have been modelled and detected in [22]. Detection and description of the athletes' running behavior is discussed in [7]. Rule-based modelling of complex basketball plays is presented in [27]. In [21], shots of basketball game are classified into one of three categories. Developing on this classification, basket events are detected when the shot sequence displays certain visual patterns. Bayes networks have been used in [15] to model and classify American football plays; however, trajectories of players and ball are entered manually, and are not automatically extracted from the video stream. In [3] automatic video annotation at an intermediate semantic level is presented: based on visual features, frames are classified respectively as "crowd," "player," or "playfield."

---

[1] A programme is said to be broadcast *as live* if it is broadcast with a very limited delay—i.e., a few hours—from its recording.

Annotation of soccer videos has been addressed by a large number of researchers. In [26], Yow et al. used mosaic images for the visualization of complete actions: players and the ball are superimposed on the background image of the playfield so that the development of the game is shown. Choi et al. [8] addressed the problem of detection and tracking of ball and players in the video sequence. The metric position of the players on the playfield was estimated using an approximation of the perspective planar transformation from the image points to the playfield model. The EU-ADMIRE project [24] has addressed modelling of semantic events in sport videos using a hierarchical rule-based approach; highlights are detected and annotated, based on low-intermediate level features extracted manually from the video stream. MPEG motion vectors were used in [18] to detect highlights. In particular, it was exploited the fact that fast camera motion is observed in correspondence of typical soccer highlights, such as shot on goal or free kick. In [13], the playfield was divided into several distinct zones: the zone is identified using patterns of the playfield lines which appear in the image. The ball position is also used to perform detection of shot on goal and corner kick highlights. Tovinkere and Qian proposed a hierarchical E-R framework for modelling the domain knowledge [23]. This scheme is suited for both team plays and individual actions, and uses a set of nested rules to check whether a particular event takes place; the model includes 3D data on the position of players and ball that are obtained from microwave sensors or multiple video cameras. Recognition of relevant soccer highlights (free kicks, corner kicks, and penalty kicks) was presented in [2]: Hidden Markov Models encoding players' distribution and camera motion were used to discriminate between the three highlights. The major weakness of the approach is in the difficulty to obtain training sets that are representative of the typical occurrences of some highlight, and, due to this, the possibility of modelling highlights that may occur with many different patterns. More recently, in [11], Ekin et al. performed highlight detection in soccer video using both shot sequence analysis and shot visual cues. In particular, they assume that the presence of highlights can be inferred from the occurrence of one or several slow motion shots and from the presence of shots where the referee and/or the goal box is framed. The method only works on edited programmes and is therefore suited only for posterity logging annotation.

In the following we present automatic detection of the principal highlights in soccer, based on the estimation of a few visual cues. We partition the playfield into different zones with slight overlapping and use the motion of the main camera as a cue for the evolution of the play. Each highlight is modelled with a Finite State Machine (FSM), where key events, defined in terms of the estimated cues, determine the transition from one state to the following. The highlight models are checked against the current observations, using a model checking algorithm. Fig. 1 provides an overview of the highlight detection engine, and of the data that are fed into the two subsystems for visual cue extraction and model checking. The system supports the detection of all the principal soccer highlights and is suited for both production and posterity logging. The work was developed within the EU-ASSAVID (Automatic Segmentation and Semantic Annotation of sports VIDeo) project, that aimed to provide a fully automated system for annotation of sports video footage. Domain experts were involved in the definition and modelling of the most relevant soccer highlights.
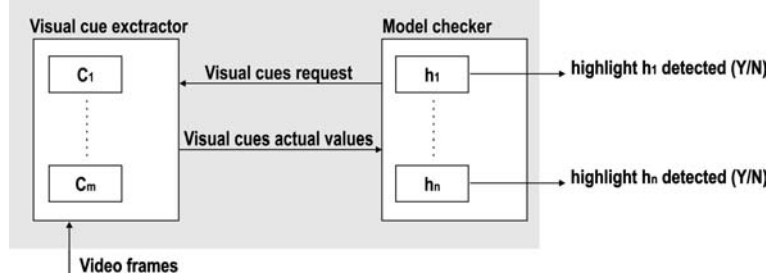
Fig. 1. Overview of principles of operation of the highlight detection engine.

The paper is organized as follows: in Section 2, we discuss the solution adopted for modelling highlights. Then, we provide details on the extraction of intermediate-level cues from the video stream (Section 3) and on model checking (Section 4). We report on experimental results in Section 5. Conclusions and future work are discussed in Section 6.

2. Highlight models and visual cues

In our approach, we model highlights using finite state machines: each highlight is described by a directed graph $\mathcal{G}^h = \langle \mathcal{S}^h, \mathcal{E}^h \rangle$, where $\mathcal{S}^h$ is the set of nodes representing the *states* and $\mathcal{E}^h$ is the set of edges representing the *events*. Events indicate transitions from one state to the other: they capture the relevant steps in the progression of the play. An event is triggered whenever a change occurs in the observed cues. The spatio-temporal analysis of the play is performed only at frames that have been previously classified as "playfield" frames [3].

As a concrete example, we consider the case of the *shot on goal* highlight. Its description provided by a domain expert is as follows:

> The player that has the ball gets closer to the opponent's goal box. He then kicks the ball towards the goal post. Eventually, the ball is either blocked by the goalkeeper, or ends into the net, or goes beyond the field end line. Alternatively, the ball gets far from the goal box.

The knowledge model obtained from this description is shown in Fig. 2. It models the temporal evolution of a specific set of observable cues that characterizes the shot on goal highlight. The ball motion—its acceleration after the player's kick, its deceleration and stop when it is blocked by the goalkeeper, its direction—and the zone of the playfield where the ball is played, are used as visual cues. They are estimated using, respectively, the camera motion and the playfield zone framed by the camera as discussed in more detail in the following section. As shown in Fig. 3a, changes in camera motion occur when the ball is kicked or stopped. The playfield region can be extracted from the frames of the sequence as shown in Fig. 3c for keyframes of Fig. 3b.

More generally, state transitions are determined by the following cues, that are directly estimated from image data: motion of the ball, currently framed playfield zone, position of the players on the playfield, color of players' uniforms. Table 1
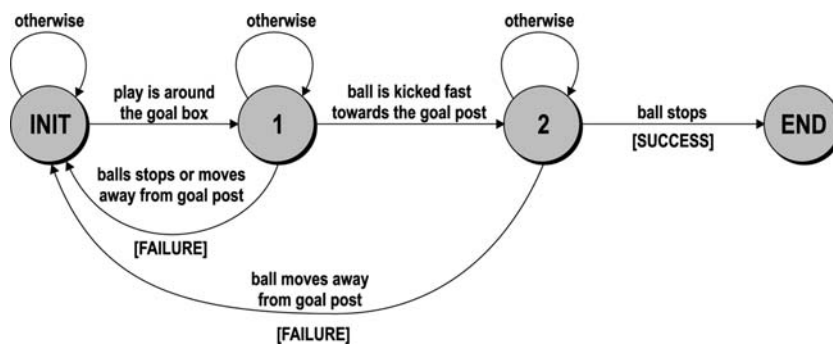
Fig. 2. The domain knowledge model captures the essence of a *shot on goal*, as described by a domain expert.
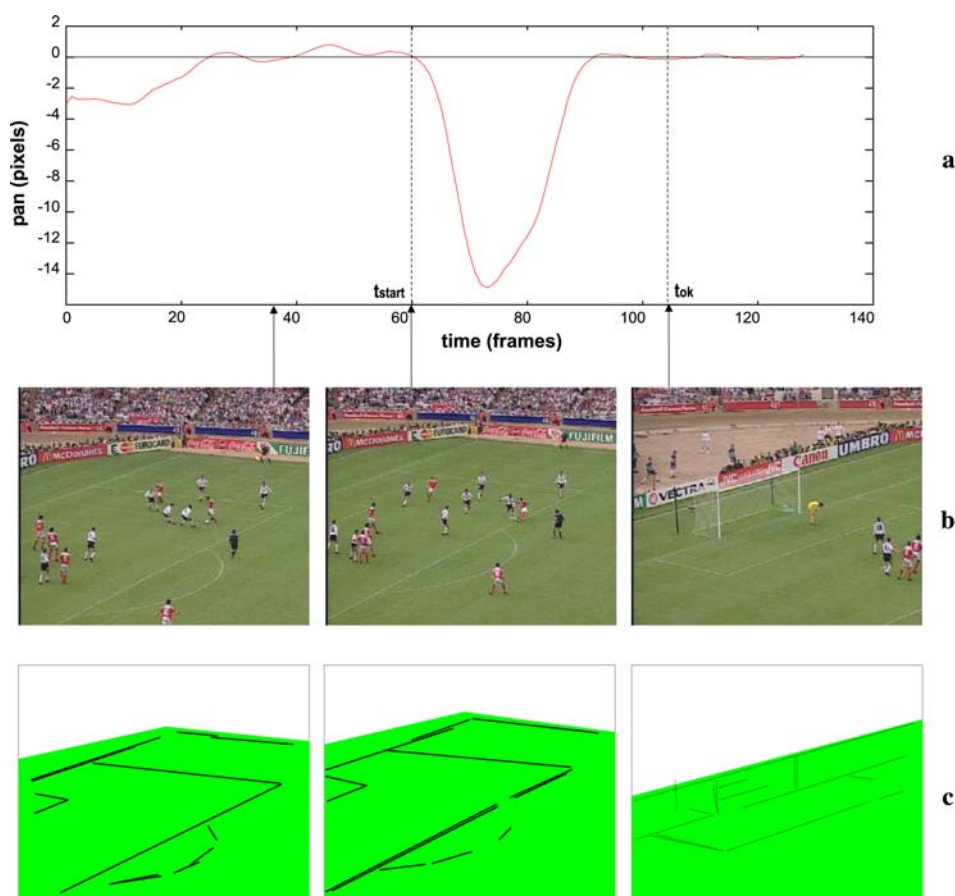

Fig. 3. Sample video sequence of a *shot on goal*. (a) Camera pan (negative pan indicates that the camera is moving towards left). (b) Keyframes of the sample sequence. (c) Playfield regions extracted from the key-frames.

Table 1
Visual cues used for the models of the highlights recognized by the system

Highlight	Visual cues				Required highlights
	Ball motion	Playfield zone	Players' position	Players' colors	
Forward pass	Y	Y	—	—	—
Shot on goal	Y	Y	—	—	—
Turnover	Y	—	—	—	—
Placed kick					
Corner	Y	Y	Y	—	—
Free kick	Y	Y	Y	—	—
Penalty	Y	Y	Y	—	—
Kickoff	Y	Y	Y	Y	—
Counterattack	—	—	—	Y	Turnover THEN forward pass

"Penalty" covers penalties that occur during the match, not those after extra time.

summarizes the visual cues that have been selected for modelling and classification of each highlight. It can be observed that highlights can be expressed in terms of other highlights (e.g., *penalty*, *corner*, and *free kick* are specializations of *placed kick*). Most of the highlights are detected using, as relevant cues, only the ball motion and the playfield zone that are estimated in every frame. Players' position and color are only used to discriminate between *placed kicks* and to identify *kickoffs*. Differently from the others, the *counterattack* highlight is modelled as a sequence of basic highlights (i.e., *turnover* followed by *forward pass*).

3. Cue estimation

The solutions adopted for the estimation of the visual cues are discussed in the following paragraphs.

3.1. Ball motion

Video producers typically use one main camera to follow the play. Due to the fact that the play always takes place next to the ball, it is fair to assume that the main camera follows the ball. Accordingly, ball motion is conveniently described in terms of pan/tilt camera motion, and estimated from the apparent image motion induced by the camera action. The validity of this assumption has been confirmed in the experiments carried out in the EU-ASSAVID project. Estimation of camera motion is easier than ball motion tracking. In fact, since the ball has a very limited image size, a robust detection of the ball is almost impossible to achieve in long field camera shots or in crowded scenes. The ball is also impossible to detect and track when it is kicked fast. Besides, even when ball tracking is successful, ball motion trajectories provide a too detailed description for the purpose of highlight detection, which only needs a coarse estimation of the direction, acceleration and location of the ball.

As in soccer videos the camera is typically in a fixed position, a 3-parameter image motion estimation algorithm capturing horizontal and vertical translations and isotropic scaling is sufficient to get a reasonable estimate of camera pan, tilt and zoom. The image motion estimation algorithm is an adaptation to the soccer domain of the algorithm reported in [4], that is based on corner tracking. As it works with a selected number of salient image locations, the algorithm can cope with large displacements due to fast camera motion. The algorithm employs deterministic sample consensus to perform a statistical motion grouping. This is particularly effective to cluster multiple independent image motions, and is therefore suitable for the specific case of soccer to separate camera motion from the motion of individual players.

3.2. Playfield zones

Given a "playfield" frame, the region of the image that represents the playfield can be roughly identified from grass color information, based on color histogram analysis. The playfield image region is then refined through a processing chain composed of K-fill, flood fill and morphological operators (erosion and dilation). A vector representation of the playfield region outline is produced.

The playfield image region is processed in order to extract an edge map which is used to obtain line segments. To this end, we rely on a growing algorithm, which produces a vector representation of the segments [20]. The playfield lines (the white lines in the playfield) are then obtained by joining together white segments that are close and collinear.

For the purpose of playfield image region classification, the playfield is divided into 12 zones Z_k, $k = 1, \ldots, 12$, six for each side. Zones are defined so that passing from one zone to the other corresponds to a new phase in the play—for instance, a defense play may change into a counterattack, or an attacking action may evolve towards the goal box. Since the main camera is usually placed in a specific position w.r.t. the playfield, each playfield zone is associated with a "typical view" taken from the main camera. Playfield zones and their typical views are shown in Fig. 4. The classification of the playfield view into one of the 12 zones is based on the attributes of the playfield image region and the playfield lines:

- *playfield region shape (RS)*. Shapes of the playfield region are distinguished into six classes, shown in Fig. 5, plus a leak hypothesis representing different (unrelevant) shapes;
- *playfield region area (RA)*. A binary value is used to indicate whether the number of pixels comprising the region is above a threshold;
- *playfield region corner position (CP)*. Four distinct values are used to discriminate between the three patterns of position of the corner farthest from the camera in Fig. 6, plus the absence of playfield corners in the image;
- *playfield line orientation (LO)*. Playfield line orientation is quantized in 4 levels, corresponding to the four orientation intervals: $[0°–10°] \cup [170°–180°)$, $[10°–60°)$, $[60°–120°)$, $[120°–170°)$. Consequently, orientations of lines detected in the frame are collected into a 4-bin histogram, and the most representative bin is chosen as the representative orientation;

Fig. 4. The six playfield zones of a half playfield (Z_7–Z_{12} are symmetrical).

Fig. 5. Typical playfield region shapes (black areas represent the playfield).

- *midfield line position (LP)*. Three distinct values are used to encode three position patterns, corresponding to the position of the midfield line in the left, central or right part of the frame. A fourth value accounts for the case where the midfield line does not appear in the frame.
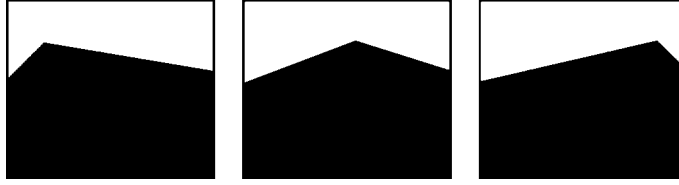
Fig. 6. Typical positions of the farthest corner in the playfield region (black areas represent the playfield).

Playfield zones are classified into one of the twelve zones using twelve independent naïve Bayes classifiers. For each frame, given the five observed attributes $\langle RS, RA, CP, LO, LP \rangle$, each classifier outputs the probability that the framed playfield image region corresponds to the classifier's zone. Following a maximum likelihood approach [15], the output probabilities of the individual classifiers are compared in order to select the highest one. This approach is justified by the fact that, in our case, the classifiers have an identical structure. Hence, large differences in the output probabilities are very likely to be significant. To filter out instantaneous misclassifications, we use a fixed length temporal window and majority voting in order to identify the playfield zone that best matches the observed variables.

3.3. Detection and metric localization of players

Blobs of individual players or groups of players are segmented out from the playfield by color differencing. Players are then identified through adaptive template matching, using an elliptical template that has the height/width ratio equal to the median of the height/width ratios of the blobs extracted. Templates are positioned at the identified players' blobs, and described by color distribution and image position, taken as the lowest point of the template (see Fig. 7, left). The player's position on
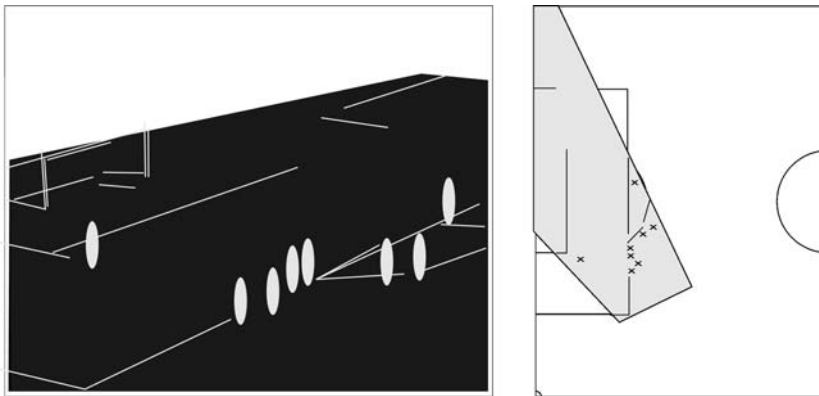
Fig. 7. Left: Players' templates positioned at the players' blobs segmented out in the image. Right: Players' locations in the playfield model, obtained by image-to-playfield backprojection of the lowest point of each template, are indicated by crosses. The visible portion of the playfield (in gray) and the players (indicated as crosses) as remapped onto the playfield model. Only the left half of the playfield model is showed here.

the playfield is computed from the projective transformation (estimated automatically at each frame) which maps a generic imaged playfield point $[x\ y]^T$ onto the real playfield point $[X\ Y]^T$ (see Fig. 7, right).

Assuming the pinhole camera projection model, the image-to-playfield transformation has the form

$$[X_1\ X_2\ X_3]^T = \mathsf{H}\,[x\ y\ 1]^T, \tag{1}$$

where $[X\ Y]^T = [X_1/X_3\ X_2/X_3]^T$ and H is a 3×3 homogeneous matrix, referred to as *planar homography*, whose eight independent entries depend on both camera position and calibration parameters [14]. To compute the position of the players on the playfield, we must compute H. Since, according to Eq. (1), each pair of corresponding points $\langle [x\ y]^T, [X\ Y]^T \rangle$ gives rise to two independent equations in the entries of H, the planar homography can in principle be estimated given a set of four or more image-to-playfield point correspondences. However, since we are provided with a set of line segments as the result of image segmentation, the homography is estimated instead using four line correspondences. Indeed, if $[a\ b\ c]^T$ such that $ax + by + c = 0$ is the image of a playfield line $[A\ B\ C]^T$, it holds

$$[a\ b\ c]^T = \mathsf{K}\,[A\ B\ C]^T, \tag{2}$$

with $\mathsf{K} = \mathsf{H}^T$. Therefore, the point transformation H is obtained from the line transformation K.

The right correspondences between image and playfield line pairs are obtained by the following deterministic consensus algorithm:
1. *Image line selection*. From all the image line segments, select a four-element subset and consider the associated line subset $\mathcal{S}_i^{\mathrm{I}} = \{[a_l\ b_l\ c_l]^T, l = 1, \dots, 4\}$;
2. *Hypothesis generation*. From all the straight lines of the playfield model (see Fig. 8), select a four-element subset $\mathcal{S}_j^{\mathrm{P}} = \{[A_l\ B_l\ C_l]^T, l = 1, \dots, 4\}$. From the
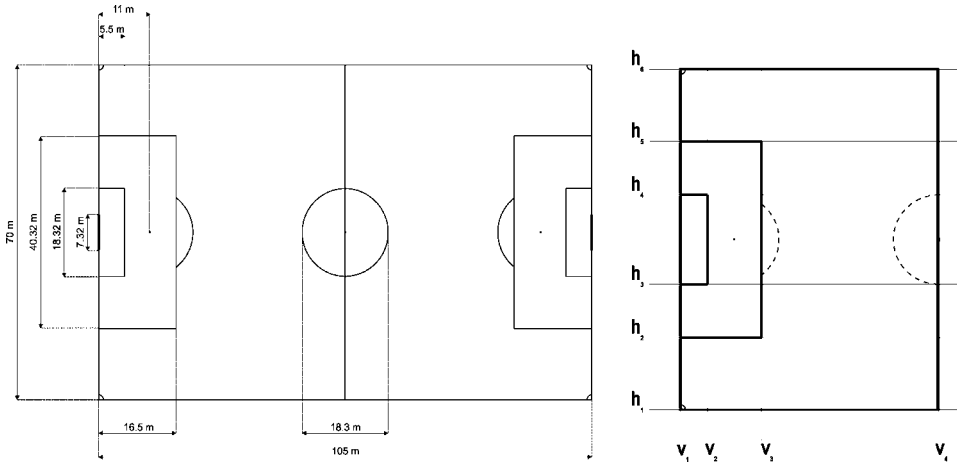

Fig. 8. Left: The complete metric model of the soccer playfield. Right: For homography estimation, only the straight lines of a half playfield are taken into account (see text).

corresponding lines in the sets $\mathcal{S}_i^{\mathrm{I}}$ and $\mathcal{S}_j^{\mathrm{P}}$, estimate the transformation K_{ij} satisfying Eq. (2);

3. *Hypothesis validation*. For all i and j, use $\mathsf{H}_{ij} = \mathsf{K}_{ij}^{\mathrm{T}}$ in Eq. (1) to remap the endpoints $\{\langle [x_\alpha^k \; y_\alpha^k]^{\mathrm{T}}, [x_\omega^k \; y_\omega^k]^{\mathrm{T}}\rangle, \; k = 1, \ldots, L\}$ of each image line segment onto the playfield model. Then evaluate the *model matching error* as $\varepsilon_{ij} = \sum_k \delta_{ijk}$, where δ_{ijk} measures the distance (evaluated by accumulation of line-point distances) of each remapped line segment to the line of the playfield model closest to it. Finally, select as a raw solution $\widehat{\mathsf{H}}$ the homography H_{ij} corresponding to the minimum model matching error;

4. *Solution refinement*. Use all the line correspondences with low segment-to-model distance under remapping with $\widehat{\mathsf{H}}$ to obtain a refined estimate $\widetilde{\mathsf{H}}$ via least squares. The refinement process corresponds to a more uniform redistribution of the overall remapping error over the entire set of image line segments.

The actual implementation of the algorithm above benefits from careful considerations about model and data characteristics, aimed at reducing dramatically the computational complexity. First of all, raw viewpoint information extracted from playfield segmentation is used to know which half of the playfield (either the left or the right one) is in view: this allows us to use a simplified model including only half of the playfield lines, namely six horizontal $\{\boldsymbol{h}_m, m = 1, \ldots, 6\}$ and 4 vertical $\{\boldsymbol{v}_n, n = 1, \ldots, 4\}$ lines (see Fig. 8, right).

Using viewpoint information and looking for dominant directions in the image line direction histogram, we are also able to classify image lines into three groups: (a) "horizontal" lines $\{\boldsymbol{m}_h, h = 1, \ldots, N_h\}$, i.e., image lines with a high probability to be projections of the $\boldsymbol{h}_m$'s; (b) "vertical" lines $\{\boldsymbol{n}_v, v = 1, \ldots, N_v\}$, with a high probability to be projections of the $\boldsymbol{v}_n$'s; (c) all the remaining lines. This preliminary line grouping has a strong impact on the computational effort during hypothesis generation, as horizontal model lines are matched only against "horizontal" lines, and vertical model lines only against "vertical" ones. Explicitly, given a subset $\mathcal{S}_i^{\mathrm{I}}$ composed of two "horizontal" and two "vertical" image lines, the number of homography hypotheses to be generated (step 2) and verified (step 3) is $\mathcal{C}(6, 2) \times \mathcal{C}(4, 2) = 90$, where $\mathcal{C}(N, 2) = N(N-1)/2$ is the number of combinations without repetitions of element pairs taken from a set of N elements. Since the number of all distinct image line subsets is $\mathcal{C}(N_h, 2) \times \mathcal{C}(N_v, 2)$, with $N_h \leqslant 6$ and $N_v \leqslant 4$, the overall number of homography hypotheses is bounded by 90^2. Values N_h and N_v are kept low by excluding from the matching process all short image line segments or image line segments that are neither "horizontal" nor "vertical." These segments are likely to be due to segmentation errors (e.g., due to the presence of non-detected players) or to be part of curvilinear portions of the model (such as the penalty arc). Each of the playfield line subsets $\mathcal{S}_j^{\mathrm{P}}$, $j \in \{1, \ldots, 90\}$ is an *ordered rectangle*, i.e., a 4-tuple $\{\boldsymbol{h}_m, \boldsymbol{h}_{m'}, \boldsymbol{v}_n, \boldsymbol{v}_{n'}\}$, with $m < m'$ and $n < n'$. Similarly, each image line subset $\mathcal{S}_i^{\mathrm{I}}$ is an ordered quadrilateral $\{\boldsymbol{m}_h, \boldsymbol{m}_{h'}, \boldsymbol{n}_v, \boldsymbol{n}_{v'}\}$, $h < h'$ and $v < v'$, the right ordering of matching candidates being explicitly inferred from the relative position of the corresponding line segments in the image. The ordering concept is crucial to eliminate the twofold specular ambiguity arising from matching unordered element pairs. In our case, the ambiguity would manifest in left/right and up/down uncertainty in the classification of "vertical" and "horizontal" image lines, respectively. The deterministic

consensus algorithm is based on a basic assumption, i.e., that the best possible homography corresponds to a minimum of model matching error. This assumption is not obvious, since there are two distinct sources of mismatch between a remapped image segment and a model line: (i) a wrong homography is being tested, i.e., the image quadrilateral is not the projection of the playfield rectangle at hand; (ii) the image segment does not correspond to any image line (e.g., it is part of the center circle). Thus, the matching strategy implicitly assumes that the matching errors of the first type are dominant, on the average, over the matching errors of the second type: this fact has been verified experimentally with an extensive test set.

Metric localization of players is used to detect the placed kicks (*corner*, *penalty*, *free kick*) nearby the goal box. Since different types of placed kicks exhibit different players' deployments, the distribution of the players' positions in specific regions of the goal box and its surroundings provides useful information in order to recognize the type of placed kick. Fig. 9 shows the region of the goal box and its surroundings
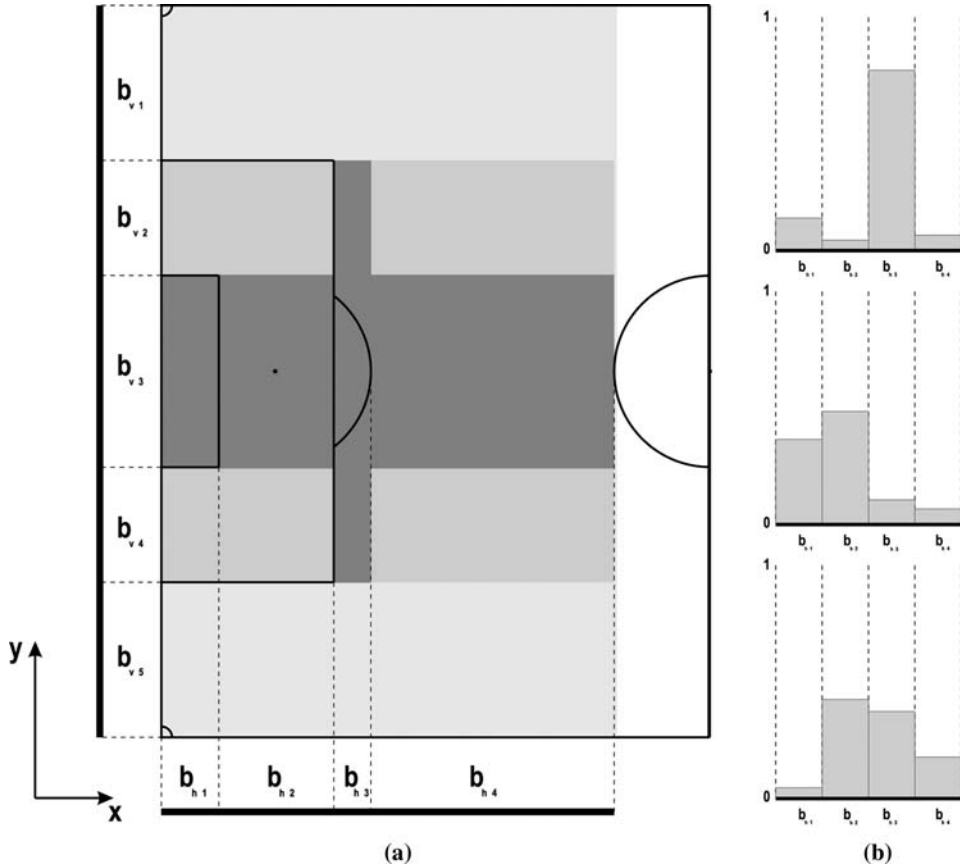

Fig. 9. (a) The goal box region and its surroundings. (b) Typical normalized distributions of players (along the *x* axis) for penalty (top), free kick (middle) and corner (bottom).
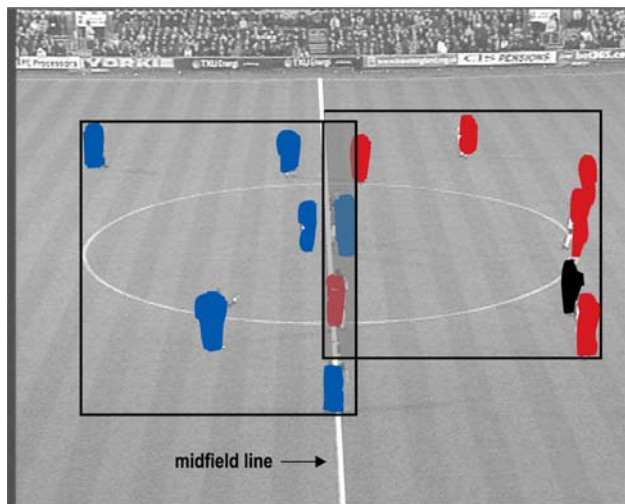
Fig. 10. Example of kickoff detection: bounding boxes of the players' clusters and midfield line.

(a), and typical players' position distributions for penalty, free kick and corner (b). Dark areas are the most relevant for the discrimination between the three types of placed kicks. Models for placed kicks exploit a cue describing players' deployment. The cue is obtained through Bayesian classifiers, whose inputs are occupation measures for each area.

Players' position is useful also for the detection of kickoffs. In fact, kickoffs are characterized by two groups of still players, each of a different team, separated by the midfield line. In this case, homography estimation and backprojection onto the playfield model can be avoided, since the separation between sets of points by a straight line in the plane is invariant to perspective projection. It is therefore sufficient to cluster players' blobs based on their colors, and check whether the clusters' bounding boxes are almost completely separated by the midfield line, directly in the image (Fig. 10).

4. Model checking

For the implementation of the highlight models in the classification engine, knowledge models are turned into operational models. Fig. 11 shows the operational models for all the soccer highlights addressed. Cues are combined through logic and relational operators to describe events on the edges of the graphs. Symbols used in the state transition expressions are explained in the legend.

The operational models are used to perform model checking. The estimated measures of the required visual cues are checked against each model in parallel. To reduce the computational costs associated with the extraction of the image features of each cue, only the cues that are needed to perform state transitions at each state
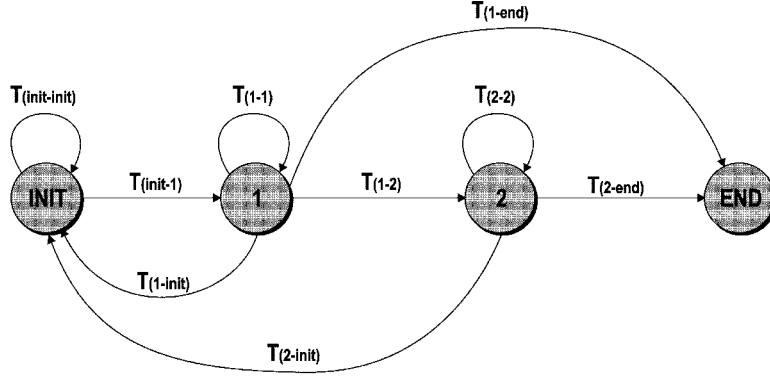
Legend:
$Z_{<i>}$: i-th playfield zone (boolean)
M: magnitude of imaged camera motion (pixel/frame)
$\mu1, \mu2$: motion threshold values (pixel/frame)

N: persistency in the current state (frame)
ν: duration threshold value (frame)
$Pd_{<j>}$: occurrence of players' position distribution (boolean)
(j=1:penalty, 2:corner, 3:free kick, 4:kickoff)

highlight state transition	Shot on goal	Penalty Corner Free kick	Forward pass	Kick off	Turnover	Counterattack
$T_{(init-init)}$	$\neg T_{(init-1)}$	$\neg T_{(init-1)}$	$\neg T_{(init-1)}$	$\neg T_{(init-1)}$	$\neg T_{(init-1)}$	$\neg T_{(init-1)}$
$T_{(init-1)}$	$(\mu1 < M < \mu2) \wedge Z2$	$(M < \mu1) \wedge Z1$	$\mu1 < M < \mu2$	$(M < \mu1) \wedge Z7$	$Z1$	turnover
$T_{(1-init)}$	$(M < \mu1) \vee (\neg Z1 \wedge \neg Z2)$	$\neg((M < \mu1) \wedge Z1)$	$M < \mu2$	$\neg((N > \nu) \wedge (PD4))$	$\neg(Z1 \vee Z5 \vee Z6)$	$N > \nu$
$T_{(1-1)}$	$\neg(T_{(1-1)} \vee T_{(1-2)})$	$\neg(T_{(1-init)} \vee T_{(1-2)})$	$\neg(T_{(1-init)} \vee T_{(1-2)})$	$\neg(T_{(1-init)} \vee T_{(1-end)})$	$\neg(T_{(1-init)} \vee T_{(1-2)})$	$\neg(T_{(1-init)} \vee T_{(1-end)})$
$T_{(1-2)}$	$(M > \mu2) \wedge Z2$	$N > \nu$	$Z6 \vee Z7$	not allowed	$Z5 \vee Z6$	not allowed
$T_{(1-end)}$	not allowed	not allowed	not allowed	$(N > \nu) \wedge (Pd4)$	not allowed	$(N < \nu) \wedge (\text{forward pass})$
$T_{(2-init)}$	$\neg Z1 \wedge \neg Z2$	$\neg(Z1 \vee Z2)$	$M < \mu2$	not allowed	$\neg(T_{(2-end)})$	not allowed
$T_{(2-2)}$	$\neg(T_{(2-init)} \vee T_{(2-end)})$	$\neg(T_{(2-init)} \vee T_{(2-end)})$	$\neg(T_{(2-init)} \vee T_{(2-end)})$	not allowed	$\neg(T_{(2-init)} \vee T_{(2-end)})$	not allowed
$T_{(2-end)}$	$M < \mu1$	$\neg(M < \mu1) \wedge Z2 \wedge Pd1$ $\neg(M < \mu1) \wedge Z2 \wedge Pd2$ $\neg(M < \mu1) \wedge Z2 \wedge Pd3$	$Z1$	not allowed	$(\mu1 < M < \mu2) \wedge (N > \nu)$	not allowed

Fig. 11. *Shot on goal*, *placed kicks*, and *forward pass* models are referred to occurrence of highlights in the left midfield (w.r.t. the camera view). *Turnover* and *counterattack* models are referred to the situation in which the team defending the left midfield gain the possess of the ball.

are estimated. Algorithm 1 presents the model checking algorithm in detail. In the main loop, the image features (e.g., line segments, players' blobs, and grass color) relevant for cue estimation are extracted from the incoming frame. For each highlight, the algorithm analyzes if the observed cue verifies the constraint associated with transitions outgoing from the current state. If a transition constraint is verified, the model state is updated. Whenever a model is checked successfully, the stream segment is annotated with the highlight and its initial and final time instants.

To reduce the computational requirements, at each frame, only the features that are required to check the transitions of the current states of the active highlight models are extracted. A reference counter $ref\_counter[f]$ tracks the number of models for which the current state requires the extraction of feature f, and is updated at each state transition $e_{i,j}^h$. Variables F_{dec} and F_{inc} contain, respectively, features that are no longer needed and features that are required by the model when entering the new state s_j^h.

Algorithm 1. Model checking algorithm.

```
main()
   for each feature f do
      ref_counter[f] = 0;   /* ref_counter[f] counts models requiring evaluation
      of f */
   for each highlight h do
      init_model(h);
   while ( ! end_of( video_stream ) )
      for each feature f do
       if( ref_counter[f] > 0 )
          compute(f);
      for each highlight h do
       if ( check_model(h) )
          annotate( m.highlight_type, m.in, m.out );
current_frame++;
   init_model(int h)
      model[h].status = INIT;
      foreach feature f do
         for each k such that ((e₀,ₖʰ ∈ ℰʰ) ∧ (e₀,ₖʰ requires f)) do
         ref_counter[f] + +;
   boolean check_model(int h)
      boolean rv = FALSE;
      if ( occurred_event( eᵢ,ⱼʰ ) )
         if ( sᵢʰ = = INIT )
          model[h].in = current_frame;
         if ( sⱼʰ = = FAIL )
          j = 0;
         else if ( sⱼʰ = = SUCCESS )
          model[h].out = current_frame;
          rv = TRUE;
          j = 0;
         Fᵢ = ⋃ₖ|ₑᵢ,ₖʰ∈ℰʰ {f|detection of eᵢ,ₖʰ requires f};
         Fⱼ = ⋃ₖ|ₑⱼ,ₖʰ∈ℰʰ {f|detection of eⱼ,ₖʰ requires f};
         F_dec = Fᵢ - Fⱼ;   /* set of features whose evaluation is no longer required */
         F_inc = Fⱼ - Fᵢ;   /* set of required features that were not evaluated so far */
         for each feature f ∈ F_dec do
          ref_counter[f] − −;
```

for each feature $f \in F_{inc}$ do
  $ref\_counter[f] + +$;
  $model[h].status = s_j^h$;
return rv;

5. Experimental results

Solutions and algorithms presented in the previous sections effectively support production logging, in that they allow highlight classification in quasi real-time. In the following, we present experimental results of highlight detection and discuss computational costs of the proposed solutions.

5.1. Highlights detection

Experiments have been carried out with videos of soccer games provided by BBC Sports Library and recorded off-air from other broadcasters. Videos were acquired from Digital Video (DV) tapes, recorded at full PAL resolution and 25 fps. The overall test set includes over 100 sequences with typical soccer highlights, of duration from 15 s to 1.5 min. The relative frequency of the different types of highlights reflects that of a typical soccer game. Table 2 shows correct, missed, and false detection for the principal soccer highlights. It can be noticed that, for most of the highlights, correct detection is over 90%.

Fig. 12 shows a case of missed detection, where the model fails to capture the current highlight of *shot on goal*: the attacking player (A) carries the ball towards the goal box (keyframes 1–3) and passes the ball to player B (keyframe 4), who is very close to the goalkeeper and the goal post. Player B shoots the ball slowly into the goal post (keyframes 5–6). This results in little camera motion, which does not allow the system to detect the highlight according to the model of *shot on goal* defined (see Fig. 11).

Turnovers display high false detection rates. *Turnover* models were in fact designed so as to allow low missed detection at the expense of a high number of false detections. In fact, *turnovers* are mainly used as a cue to detect *counterattacks*—*counterattacks* are defined as a *turnover* followed by a *forward pass*—that are much more significant. In this perspective, false *turnover* detections do not

Table 2
Highlight detection rate for the principal highlights

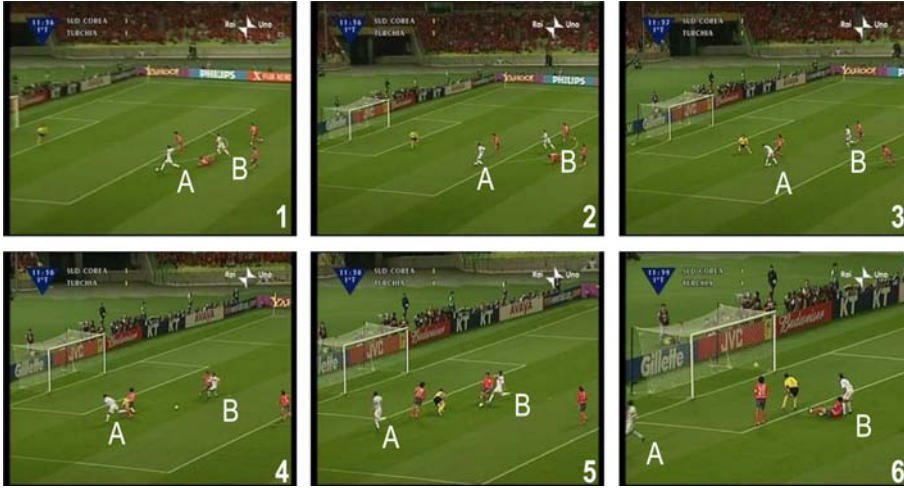| Highlight	Detected	Correct	Missed	False
Forward pass	39	35	2	4
Shot on goal	19	15	2	4
Placed kick	15	14	1	0
Turnover	20	10	1	10
Counterattack	6	5	1	1
Kickoff	4	4	0	0

Fig. 12. Case of missed detection of a *shot on goal* (keyframes).

represent a serious problem, as they can be discarded later when checking for the *forward pass*.

Table 3 reports results for a second experiment focussing on identification of different types of placed kicks. The test set included video sequences with 60 placed kicks, 20 for each one of the three classes (penalty, corner, free kick). It can be noticed that correct detection is in all cases over 95%. This high detection rate is mainly due to the good precision attained in the evaluation of the players' position using the planar homography.

Fig. 13 shows a video sequence and the on-line detection of its principal highlights (*shot on goal*, *placed kick*, *forward pass*, and *turnover*). A dot inside a circular button indicates that a highlight is hypothesized; if the hypothesis is confirmed, i.e., the highlight is detected, a $\sqrt{}$ mark is displayed inside the button. Conversely, if the hypothesis is rejected, an $\times$ mark is displayed.

5.2. Computational costs: case study

According to the model-driven strategy described in Section 4 for model checking, at each frame, for a given highlight, only the cues that are required to trigger any transition from the current state are actually estimated. Therefore, for a given highlight h, the corresponding computational cost per frame is

Table 3
Highlight detection rate for placed kicks

	Detected	Correct	Missed	False
Penalty	18	17	0	1
Corner	19	18	1	1
Free kick	18	17	1	1

Fig. 13. A video sequence and the output of the highlight detection engine. Highlights are first hypothesized (●), and hypotheses are then either confirmed (√) or rejected (×).

Table 4
Required cues, computational costs and estimated state probabilities for each state of the *placed kick* model

State	Required cues	$\mathcal{C}(s)$	$P(s)$
0	Playfield zone, ball motion	$2c$	0.783
1	Playfield zone, ball motion	$2c$	0.150
2	Playfield zone, ball motion, players' positions	$3c$	0.065
3	—	0	0.002

$$\mathcal{C}_h = \sum_{s=1}^{S_h} \mathcal{C}(s) \cdot P(s), \tag{3}$$

where S_h is the total number of states for the highlight model, $\mathcal{C}(s)$ is the computational cost for the estimation of all cues required at state s, and $P(s)$ is the probability of state s. It follows that the computational cost for a sequence of N frames is $N \times \mathcal{C}_h$. Model-driven cue evaluation has a significant computational advantage over a brute-force approach where all cues are estimated at each frame regardless of their actual relevance for the current state. In fact, the computational cost of brute-force model checking is in any case equal to $\max_s \mathcal{C}(s)$.

Table 4 shows the cues required, the computational costs and the probabilities for each state of a *placed kick* highlight. It is assumed that all cues have the same computational cost c. As shown in Fig. 11, the model of a *placed kick* requires the estimation of two cues at states 0 (INIT) and 1, three cues at state 2, and 0 cues at state 3 (END). State probabilities have been inferred experimentally from the test set by evaluating the relative frequencies of model states during the model checking phase. According to Eq. (3), the overall cost per frame for the placed kick using the model-driven strategy is therefore equal to $2c \times 0.783 + 2c \times 0.150 + 3c \times 0.065 = 2.061c$. The corresponding cost for the brute-force strategy is $3c$, with a performance degradation of about 30%. The computational gain obtained with the proposed model-driven strategy proves useful for both production and posterity logging, in that it yields a smaller annotation delay and therefore allows video footage to be available for re-use within short time. Our prototype runs on a single processor PC (P4 2Ghz, 512Mb ram, SCSI disks). Evaluation of the computational cost c in terms of processing time per frame, yields an average of about 0.06 s/frame. For a video sequence of a *placed kick* of 5 s, the required processing time is therefore about 15.5 s. This reflects the average performance of the system, for which the processing rate is about 1/3 the real time frame rate (i.e., 3 s of processing for each second of video). The system meets the ''as live'' requirement for annotation mentioned in Section 1.

6. Conclusions

In this paper, we have presented a novel approach for automatic semantic annotation of soccer video. The annotation engine detects the principal highlights of soccer by checking a limited number of observed visual cues against highlight models,

that are defined as finite state machines. The solution proposed is suitable for both production logging and posterity logging. In both cases, objective annotations provided by the system can be complemented by subjective remarks (e.g., a "nice goal") provided by humans.

Results that have been presented show that all the principal highlights of soccer are detected with great accuracy. With respect to previous work on soccer highlights detection, the improvements provided by this solution are both in the number of significant highlights detected by the system, and in the higher accuracy achieved. Moreover, the use of FSM models instead of learning-based approaches has the advantage of avoiding erroneous classifications due to incomplete training sets. In that we use FSM models to describe highlights and visual cues combinations to define transitions from one state to the other of the FSMs the approach can be in principle extended to other domains, provided that visual cues specific of these domains are appropriately selected so as to reflect meaningful changes of phases in the play.

With edited streams, as usually available for posterity logging, highlight models can be enhanced by including new cues—like voice comments, crowd cheering, replay and text captions—with the goal of enriching the annotation and improving the accuracy of model checking. Research on the semantic annotation of edited soccer streams for posterity logging is presently under development.

References

[1] P. Aigrain, P. Joly, The automatic real-time analysis of film editing and transition effects and its applications, Comput. Graph. 18 (1) (1994) 93–103.

[2] J. Assfalg, M. Bertini, A. Del Bimbo, W. Nunziati, P. Pala, Soccer highlights detection and recognition using HMMs, in: Proc. Internat. Conf. on Multimedia and Expo (ICME2002) 2002, pp. 825-828.

[3] J. Assfalg, M. Bertini, C. Colombo, A. Del Bimbo, Semantic annotation of sports videos, IEEE Multimedia 9 (2) (2002) 52–60.

[4] G. Baldi, C. Colombo, A. Del Bimbo, A compact and retrieval-oriented video representation using mosaics, in: Proc. 3rd Internat. Conf. on Visual Information Systems VISual99, Springer Lecture Notes on Computer Science, Amsterdam, The Netherlands, June 1999, pp. 171–178.

[5] M. Bertini, A. Del Bimbo, P. Pala, Content-based indexing and retrieval of TV news, Pattern Recognition Lett. 22 (5) (2001) 503–516.

[6] D. Chen, K. Shearer, H. Bourlard, Video OCR for Sport Video Annotation and Retrieval, in: Proc. 8th IEEE Internat. Conf. on Mechatronics and Machine Vision in Practice, 2001.

[7] F. Cheng, W.J. Christmas, J, Kittler, Detection and description of Human Running Behaviour in Sports Video Multimedia Database, in: Proc. ICIAP, 2001.

[8] S. Choi, Y. Seo, H. Kim, K.-S. Hong, Where are the ball and players?: Soccer Game Analysis with Color-based Tracking and Image Mosaick, in: Proc. Internat. Conf. Image Analysis and Processing (ICIAP'97), Springer Lecture Notes on Computer Science, 1997.

[9] C. Colombo, A. Del Bimbo, P. Pala, Semantics in visual information retrieval, IEEE MultiMedia 6 (3) (1999) 38–53.

[10] N. Dimitrova, T. McGee, H. Elenbaas, J. Martino, Video content management in consumer devices, IEEE Trans. Knowledge Data Eng. 10 (6) (2001) 995–998.

[11] A. Ekin, A. Murat Tekalp, R. Mehrotra, Automatic Soccer Video Analysis and Summarization, IEEE Trans. Image Process. 12 (7) (2003) 796–807.

[12] U. Gargi, R. Kasturi, S.H. Strayer, Performance characterization of video-shot-change detection methods, IEEE Trans. Circuits Syst. Video Technol. 10 (1) (2000).

[13] Y. Gong, L.T. Sin, C.H. Chuan, H. Zhang, M. Sakauchi, Automatic Parsing of TV Soccer Programs, in: Proc. Internat. Conf. on Multimedia Computing and Systems (ICMCS'95), Washington, DC, May 15–18, 1995.

[14] R. Hartley, A. Zisserman, Multiple View Geometry in Computer Vision, Cambridge University Press, Cambridge, 2000.

[15] S.S. Intille, A.F. Bobick, Recognizing planned, multi-person action, Comput. Vis. Image Understand. (1077–3142) 81 (3) (2001) 414–445.

[16] M. Irani, P. Anandan, J. Bergen, R. Kumar, S. Hsu, Mosaic Representations of video sequences and their applications, Signal Process.: Image Commun. 8 (4) (1996) (special issue on Image and Video Semantics: Processing, Analysis, and Application).

[17] J. Kittler, K. Messer, W.J. Christmas, B. Levienaise-Obadia, D. Koubaroulis, Generation of semantic cues for sports video annotation, in: Proc. ICIP 2001.

[18] R. Leonardi, P. Migliorati, Semantic indexing of multimedia documents, IEEE MultiMedia 9 (2) (2002) 44–51.

[19] R. Lienhart, Indexing and retrieval of digital video sequences based on automatic text recognition, in: Proc. 4th ACM Internat. Multimedia Conf., 1996.

[20] R.C. Nelson, Finding line segments by stick growing, IEEE Trans. PAMI 16 (5) (1994) 519–523.

[21] S. Nepal, U. Srinivasan, G. Reynolds, Automatic detection of 'Goal' segments in basketball videos, Proc. ACM Multimedia (2001) 261–269.

[22] G. Sudhir, J.C.M. Lee, A.K. Jain, Automatic classification of Tennis video for high-level content-based retrieval, in: Proc. Internat. Workshop on Content-Based Access of Image and Video Databases CAIVD'98, 1998, pp. 81–90.

[23] V. Tovinkere, R.J. Qian, Detecting semantic events in Soccer Games: towards a complete solution, in: Proc. Internat. Conf. on Multimedia and Expo ICME 2001, pp. 1040–1043.

[24] A. Woudstra, D.D. Velthausz, H.J.G. de Poot, F. Moelaert El-Hadidy, W. Jonker, M.A.W. Houtsma, R.G. Heller, J.N.H. Heemskerk, Modeling and retrieving Audiovisual Information—A Soccer Video Retrieval System, in: Proc. 4th Internat. Workshop on Multimedia Information Systems (MIS'98), Springer Lecture Notes on Computer Science, vol. 1508, Istanbul, Turkey, September 1998, pp. 161–173.

[25] M.M. Yeung, B.L. Yeo, Time-constrained clustering for segmentation of Video into Story Units, in: Proc. Internat. Conf. on Pattern Recognition ICPR'96, 1996, pp. 375–380.

[26] D. Yow, B.-L. Yeo, M.Yeung, B. Liu, Analysis and presentation of Soccer highlights from digital video, in: Proc. 2nd Asian Conf. on Computer Vision (ACCV'95), 1995.

[27] W. Zhou, A. Vellaikal, and C.C.J. Kuo, Rule-based video classification system for basketball video indexing, in: Proc. ACM Multimedia 2000 Workshop, 2000, pp. 213–216.

[28] H.J. Zhang, A. Kankanhalli, S.W. Smoliar, Automatic partitioning of video, Multimedia Syst. 1 (1) (1993) 10–28.